Neural Computing and Applications (2021) 33:12777–12789
https://doi.org/10.1007/s00521-021-05922-x

ORIGINAL ARTICLE

# Trajectory tracking control for underactuated unmanned surface vehicle subject to uncertain dynamics and input saturation

Dongdong Mu[1] · Guofeng Wang[1] · Yunsheng Fan[1]

Received: 29 August 2020 / Accepted: 11 March 2021 / Published online: 27 May 2021


**Abstract**

In this paper, one concerns with the problem of trajectory tracking control for an underactuated unmanned surface vehicle subject to uncertain dynamics and input saturation. A first-order sliding surface and a second-order sliding surface are hired to design surge control law and yaw control law, respectively, which together form an underactuated trajectory tracking controller. Furthermore, the potential input saturation problem is solved through an auxiliary design system. Neural shunting model is introduced into the design of the controller to avoid the increase in calculation caused by variable derivation. The minimum learning parameter method of neural network replaces the traditional multilayer neural network to compensate uncertain dynamics and time-varying disturbances, which further reduces the computational burden of the controller. Besides, two adaptive robust terms are introduced to further enhance the robustness of the trajectory tracking system. Finally, comparative simulation experiments are carried out to verify the universality and superiority of the trajectory tracking control strategy.

**Keywords** Underactuated unmanned surface vehicle · Trajectory tracking · Uncertain dynamics · Input saturation

## 1 Introduction

Unmanned surface vehicle (USV) can perform dangerous or inappropriate tasks with full autonomy or human intervention, which not only protects the personal safety of staff but also saves human and material costs to a large extent [1–4]. It is precisely because of its excellent characteristics that USV has been listed as a key research object in the field of marine armaments by governments all over the world, especially the military. Among the many advantages of USV, track tracking is the basis of many other advanced functions, which can be divided into two categories: path following and trajectory tracking [5–8]. The main difference between path following and trajectory tracking is that path following has nothing to do with time, that is to say, it can only travel along a predetermined route without special requirements for time; trajectory tracking is time-dependent, that is, USV needs to arrive at a specific place at a specific time, and there is a strict correspondence between location and time. From the perspective of engineering implementation, it is more strict and difficult to achieve than path following task, but it is of great significance.

Trajectory tracking is a focus problem in the field of motion control of unmanned surface vehicle, and it plays an important role in USV formation control and reconnaissance. For example, in the execution of special tasks such as enemy ship tracking, USV needs to go to a specific location at a specific time according to the preset trajectory. In addition, USV is a typical underactuated system because it is not equipped with side thruster, that is, it is uncontrollable in the lateral direction [9, 10]. In order to realize the trajectory tracking of underactuated USV, Godhavn et al. [11] proposed a method based on backstepping and feedback linearization and designed the underactuated trajectory tracking controller but did not consider the influence of external disturbance on the controller. In [12], a globally asymptotically stable trajectory tracking controller for underactuated ship was proposed based on the backstepping algorithm with integral, which can achieve better control effect when the environmental disturbance is unknown or slowly varying. However, the method of [12]

✉ Dongdong Mu
ddmu@dlmu.edu.cn

[1] School of Marine Electrical Engineering, Dalian Maritime University, Dalian 116026, China

is to suppress the external interference through the robustness of the algorithm, which can not effectively compensate the environmental interference. In [13], the backstepping method was used to design the trajectory tracking controller of unmanned aerial vehicle, and the disturbance observer was used to estimate and compensate the time-varying external disturbance. However, in the process of USV driving on the sea, in addition to the constant interference of external factors such as wind, wave and current, its speed and moment of inertia also change, which will lead to some unknown dynamic changes of the model. Neural network [14, 15] and fuzzy logic [16, 17] have been proved to have the ability to approximate continuous functions arbitrarily, and they have been widely used in engineering applications and theoretical verification. In view of the fact that underactuated ships only have longitudinal thrust and steering torque, Li et al. [18] proposed a new point-to-point control task and estimated the unknown problems in the model through radial basis function neural network and compensates them effectively. Combining neural network adaptive technology with backstepping method, the control method proposed in [19] can track the desired trajectory under error constraints and ensure that the system is uniformly bounded under certain actuator faults. However, [18] nor [19] considered the problem of "computational explosion" of backstepping, that is, when the virtual control law needs multiple derivatives, the design of the controller will become very complex. In [20], the dynamic surface algorithm was introduced into the design of controller to estimate the derivative of virtual control law, so as to avoid the "calculation explosion" problem caused by multiple derivation of virtual control law. However, as a kind of multilayer neural network, radial basis function neural network undoubtedly increases the burden of controller. In order to effectively solve this problem, Professor Yang proposed the least learning parameter method based on the small gain theory, which can not only avoid the singular problems of other adaptive algorithms, but also reduce the number of adaptive parameters to a minimum, greatly reducing the amount of calculation [21]. Paper [22] designed a robust adaptive trajectory tracking controller for underactuated USV, and neural network least learning parameter method was introduced into the controller design to estimate and compensate the external time-varying disturbance and unknown dynamics in the model. Nevertheless, none of the above literature works considered an important problem-input saturation. Input saturation is a potential problem in controller design. If not taken into account, the instruction value of the controller may exceed the maximum range that the actuator can provide, which will lead to the instability or collapse of the controlled system [23, 24].

In this paper, motivated by the above-mentioned observations, a general trajectory tracking control strategy, which is performed by using sliding mode control theory, neural shunting model, minimum learning parameter method for neural network, adaptive technology, auxiliary design system is developed for underactuated USV subject to uncertain dynamics and time-varying disturbances. The main contributions of paper note can be summarized as follows:

(1) A novel trajectory tracking control scheme for underactuated USV is proposed, which uses first-order sliding mode and second-order sliding mode to stabilize surge velocity error and sway velocity error, respectively. Minimum learning parameter method of neural network is employed to estimate and compensate uncertain dynamics and unmeasurable external disturbances in real time, and adaptive technology is used to further offset the compensation error of neural network. In addition, auxiliary design system is used to solve the potential input saturation problem.

(2) This paper improves the robustness of the trajectory tracking control strategy from three aspects: The sliding mode control method itself has strong robustness; the neural network online real-time compensation uncertain dynamics and unmeasurable external disturbances increase the anti-interference ability; the adaptive robust term offsets the compensation error of the neural network, to further increase the robustness of the control strategy.

(3) This paper reduces the complexity of the trajectory tracking control strategy from three aspects: The neural shunting model is hired to avoid the problem of "explosion of computation"; minimum learning parameter method for neural network with less computation takes the place of traditional multilayer neural network to compensate uncertain dynamics and time-varying disturbances; uncertain dynamics and time-varying disturbances are treated as a whole rather than as compensation alone.

This paper is organized as follows. In Sect. 2, the problem formulations are introduced. Preparatory knowledge is introduced in Sect. 3. The design process of the control strategy is given in Sect. 4. In Sect. 5, analysis of system stability is formulated. Numerical simulations and comparative experiments are provided in Sect. 6. Finally, Sect. 7 summarizes the full text and introduces the future research content.

## 2 Problem formulation

The motion state of USV in actual navigation is very complex, which mainly includes six degrees of freedom: surge velocity $u$, sway velocity $v$, yaw rate $r$, heave velocity $w$, rolling rate $p$ and pitching rate $q$ [25, 26]. Earth-fixed frame and Body-fixed frame are usually used to describe the relationship between them, which can be referred to in Fig. 1.

$(x, y)$ is used to describe the position coordinates of USV, $\psi$ stands for the course of USV. The kinematics and dynamics equations of unmanned aerial vehicles are described as (1) and (2).

$$\begin{cases} \dot{x} = u\cos(\psi) - v\sin(\psi) \\ \dot{y} = u\sin(\psi) + v\cos(\psi) \\ \dot{\psi} = r \end{cases} \tag{1}$$

$$\begin{cases} m_{11}\dot{u} - m_{11}f_u + \nabla_u = \tau_u + b_u \\ m_{22}\dot{v} - m_{22}f_v + \nabla_v = b_v \\ m_{33}\dot{r} - m_{33}f + \nabla_r = \tau_r + b_r \end{cases} \tag{2}$$

where $f_u = \frac{m_{22}}{m_{11}}vr - \frac{d_{11}}{m_{11}}u$, $f_v = -\frac{m_{11}}{m_{22}}ur - \frac{d_{22}}{m_{22}}v$ and $f_r = \frac{m_{11}-m_{22}}{m_{33}}uv - \frac{d_{33}}{m_{33}}r$, $\nabla_u = \Delta_u f_u$, $\nabla_v = \Delta_v f_v$ and $\nabla_r = \Delta_r f_r$ represent the uncertain dynamics of each item, respectively, $\Delta_u$, $\Delta_v$ and $\Delta_r$ stand for uncertain parameters, $\tau_u$ and $\tau_r$ are used to describe the force and moment that cause the USV to forward and turn, respectively, $b_u$, $b_v$ and $b_r$ represent the unmeasurable time-varying external disturbances in all directions.

***Remark 1*** $\tau_u$ and $\tau_r$ are bounded by the physical limitations of the actuator, which is the input saturation problem. The specific physical limitations can be described as $\tau_{u\min} \le \tau_u \le \tau_{u\max}$, $\tau_{r\min} \le \tau_r \le \tau_{r\max}$, where $\tau_{u\max} \ge 0$, $\tau_{u\min} \le 0$, $\tau_{r\max} \ge 0$ and $\tau_{r\min} \le 0$. Although $\tau_{u\min}$ and $\tau_{r\min}$ are constants less than zero, the minus sign only indicates the direction of force and moment.

**Assumption 1** Assume that uncertain dynamics and unmeasurable time-varying external disturbances are bounded. $|\Delta_u| \le \Delta_{u\max}$, $|\Delta_v| \le \Delta_{v\max}$, $|\Delta_r| \le \Delta_{r\max}$, $|b_u| \le b_{u\max}$, $|b_v| \le b_{v\max}$, $|b_r| \le b_{r\max}$, where $\Delta_{u\max} > 0$, $\Delta_{v\max} > 0$, $\Delta_{r\max} > 0$, $b_{u\max} > 0$, $b_{v\max} > 0$ and $b_{r\max} > 0$.

*Control objective* The practical conditions considered in this paper include underactuated model, uncertain dynamics, unmeasurable time-varying external disturbances caused by the wind, wave and currents and input saturation. The control objective is to propose a practical underactuated trajectory tracking controller (design control laws $\tau_u$ and $\tau_r$) to deal with the above-mentioned issues, such that the USV (2) can track the pre-set trajectory $(x_d, y_d)$.

***Remark 2*** $x_d$ and $y_d$ are functions of time, respectively, and they are continuous and differentiable.

## 3 Preparatory knowledge

### 3.1 Neural shunting model

In essence, neural shunting model belongs to the basic knowledge in the field of neurology, and its significance is to describe the stress response of neurons to external stimuli. The specific form of neural shunting model is (3).

$$\dot{\beta} = -A\beta + (B - \beta)f(\alpha) - (D + \beta)g(\alpha) \tag{3}$$

where $\alpha$ and $\beta$ are the input and output of neural shunting model, respectively, $A$, $B$ and $D$ are the corresponding

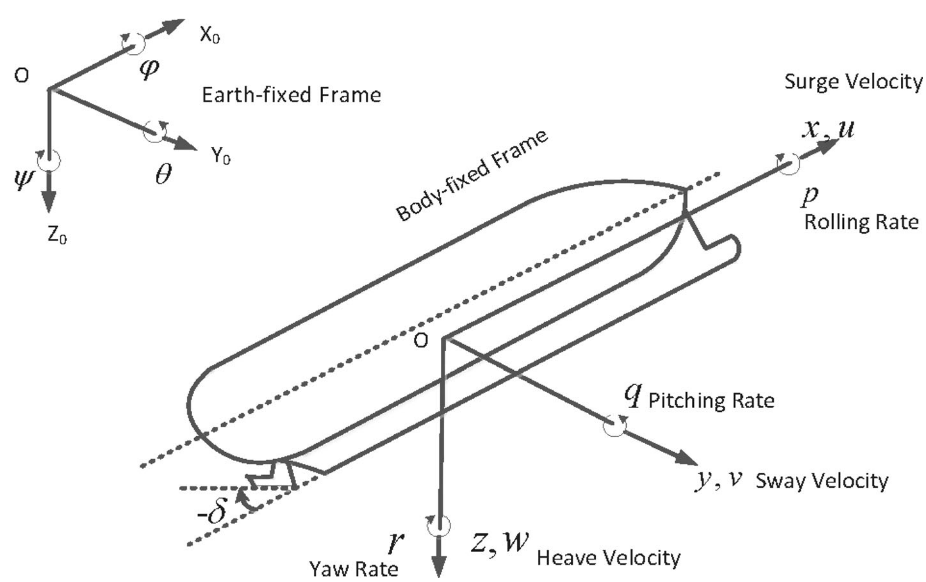


**Fig. 1** Earth-fixed frame and Body-fixed frame

positive parameters, $f(\alpha)$ and $g(\alpha)$ are valve functions, which can be expressed as: $f(\alpha) = \max\{\alpha, 0\}$ and $g(\alpha) = \max\{-\alpha, 0\}$. Neural shunting model has been widely used in many areas such as robot path planning, tracking and motor control, and so on [27].

### 3.2 Minimum learning parameter method for neural network

In the field of control theory and control engineering, the universal approximation ability of neural network is often employed to deal with uncertainties in the model and unknown functions. For a continuous function $f(x)$, it can be representated as (4) according to the universal approximation ability.

$$f(x) = W^T h(x) + \varepsilon \tag{4}$$

where $x \in \Omega_x$, $\Omega_x$ is a compact set of $R^m$, $W$ is an adaptive weight variable, $h(x)$ represents Gauss function, $\varepsilon$ stands for approximation error, and its upper bound is $\bar{\varepsilon}$, $\bar{\varepsilon} > 0$.

However, the neural network represented by RBF is a multilayer neural network, but it will undoubtedly increase the complexity of the control law, which is the so-called dimension disaster problem. In order to solve this problem effectively, Professor Yang proposed a minimum learning parameter method based on the small gain theory, which can not only avoid the singularity of other adaptive algorithms, but also reduce the number of adaptive parameters to a minimum, which greatly reduces the amount of calculation [28]. The essence of minimum learning parameter method for neural network is to replace $\|W\|$ with a constant $\phi$. $\hat{\phi}$ is the estimated value of $\phi$ and its estimated error is $\tilde{\phi} = \hat{\phi} - \phi$. The remarkable advantages of the minimum learning parameter method are: (1) reducing the self-learning parameter to one, which reduces the difficulty of controller implementation; (2) solving the "dimension disaster" problem and reducing the computational burden of the controller.

### 3.3 Auxiliary design system

Input saturation is a potential problem for any control system. If this problem is ignored, the input calculated by the control strategy may exceed the maximum output range of the actuator, which will lead to the weakening of the control effect and even the collapse of the controlled system. Input saturation problem can be described as

$$\tau = \begin{cases} \tau_{\max}, & if\ \tau_0 > \tau_{\max} \\ \tau_0, & if\ \tau_{\min} \le \tau_0 \le \tau_{\max} \\ \tau_{\min}, & if\ \tau_0 < \tau_{\min} \end{cases} \tag{5}$$

where $\tau$ is the final control input considering the input saturation problem, $\tau_0$ is the control input calculated by the control strategy without considering the input saturation problem, $\tau_{\max}$ and $\tau_{\min}$ are the maximum and minimum values that the actuator can provide, respectively. Based on this, Chen proposes an auxiliary design system to analyze potential input saturation problems [29]. The specific form of auxiliary design system can be expressed as

$$\dot{\Phi} = \begin{cases} -K_e\Phi - \dfrac{|S \cdot \Delta\tau| + 0.5\Delta\tau^2}{\Phi^2} \cdot \Phi + \Delta\tau, & |\Phi| \ge \xi \\ 0, & |\Phi|\xi \end{cases} \tag{6}$$

where $K_e$ is a positive parameter to be designed, $\Phi$ is a new auxiliary variable introduced, $S$ represents an error variable, $\xi$ is a small constant, $\Delta\tau = \tau - \tau_0$.

## 4 Control strategy

Compared with the conventional control strategy, the main difference between the sliding mode variable structure control is that it contains a control discontinuity, that is, a switching characteristic that can change the system structure according to an appropriate law. Through the discontinuity of this control, the state trajectory can be designed according to the required requirements, and under certain conditions, the system can make high-frequency, small-amplitude reciprocating motion along this trajectory. This motion is called sliding mode motion. The sliding mode is independent of the parameters and disturbances of the system and can be designed according to different requirements. Therefore, the system with sliding mode motion has excellent anti-interference and parameter robustness. At present, the theory of sliding mode control has been widely used in various fields such as aviation, robots, drones and has achieved good application results [30, 31].

In this Section, a first-order sliding mode and a second-order sliding mode are employed separately to design surge control law and yaw control law. In order to better understand the design idea of this paper, the structure of the trajectory tracking control strategy is described in Fig. 2.

$x_d$ and $y_d$ represent the position of reference trajectory. $u_d$ and $v_d$ denote the reference surge speed and sway velocity. $u_e$ and $v_e$ represent the error between the reference speed and the actual speed. Specific details will be introduced in the following controller design.

### 4.1 Surge control law

Define trajectory tracking error variables $x_e$ and $y_e$.

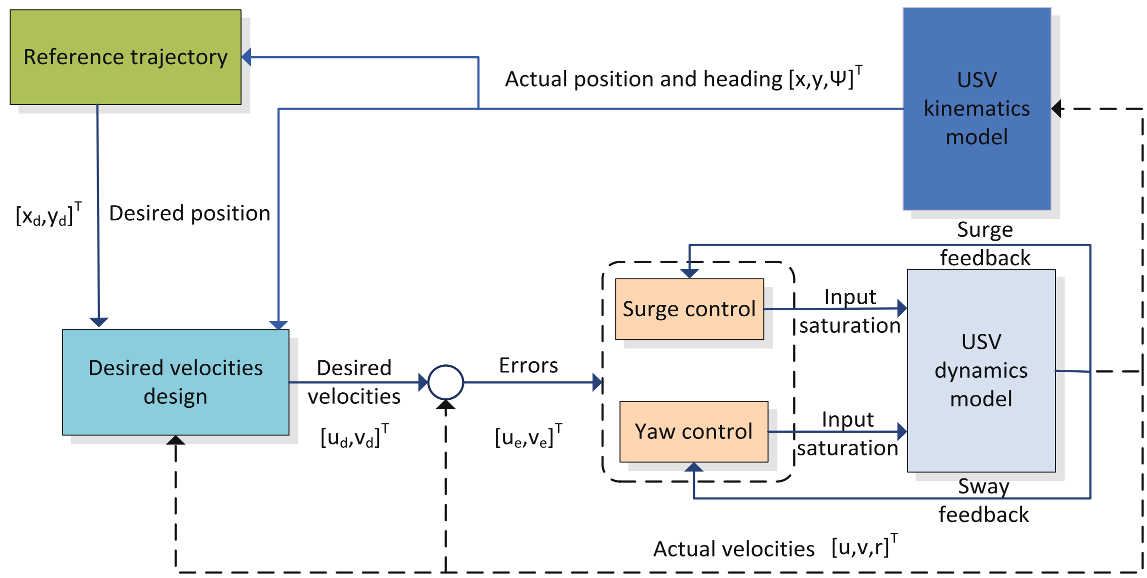


**Fig. 2** The structure of trajectory tracking control strategy

$$\begin{cases} x_e = x - x_d \\ y_e = y - y_d \end{cases} \tag{7}$$

whose time derivative along (1) can be described as

$$\begin{bmatrix} \dot{x}_e \\ \dot{y}_e \end{bmatrix} = \begin{bmatrix} \cos\psi & -\sin\psi \\ \sin\psi & \cos\psi \end{bmatrix} \begin{bmatrix} u \\ v \end{bmatrix} - \begin{bmatrix} \dot{x}_d \\ \dot{y}_d \end{bmatrix} \tag{8}$$

Meanwhile, define speed tracking error variables $u_e$ and $v_e$.

$$\begin{cases} u_e = u - u_d \\ v_e = v - v_d \end{cases} \tag{9}$$

The time derivative of (9) along (8) can be described as

$$\begin{bmatrix} \dot{u}_e \\ \dot{v}_e \end{bmatrix} = \begin{bmatrix} rv_e \\ -ru_e \end{bmatrix} + \begin{bmatrix} \cos\psi & \sin\psi \\ -\sin\psi & \cos\psi \end{bmatrix} \begin{bmatrix} \ddot{x}_e + k\dot{x}_e \\ \ddot{y}_e + k\dot{y}_e \end{bmatrix} \tag{10}$$

Assuming $(u_d, v_d)$ is associated with $(x_d, y_d)$ and $(x_e, y_e)$, it can be described as

$$\begin{cases} u_d = \cos\psi\dot{x}_d + \sin\psi\dot{y}_d - k\cos\psi x_e - k\sin\psi y_e \\ v_d = -\sin\psi\dot{x}_d + \cos\psi\dot{y}_d + k\sin\psi x_e - k\cos\psi y_e \end{cases} \tag{11}$$

where $k$ is a positive parameter to be designed.

The derivative of (11) can be described as

$$\begin{cases} \dot{u}_d = \cos\psi\ddot{x}_d + \sin\psi\ddot{y}_d + v_d r - k\cos\psi\dot{x}_e - k\sin\psi\dot{y}_e \\ \dot{v}_d = -\sin\psi\ddot{x}_d + \cos\psi\ddot{y}_d - u_d r + k\sin\psi\dot{x}_e - k\cos\psi\dot{y}_e \end{cases} \tag{12}$$

In the next step, a first-order sliding mode will be introduced to design surge control law $\tau_u$ to converge the speed tracking error $u_e$. Meanwhile, it can be seen from (12) that $\dot{u}_d$ is quite complex. To avoid this problem (explosion of computation), neural shunting model is used to avoid the derivation of $u_d$ to reduce the computational burden of the controller.

Let $u_d$ pass through the neural shunting model (3) to avoid the derivation of $u_d$, and one has

$$\dot{\beta}_d = -A\beta_d + (B - \beta_d)f(u_d) - (D + \beta_d)g(u_d) \tag{13}$$

where $A$, $B$ and $D$ have the same meaning as defined in (3).

Neural network minimum learning parameter method is introduced into the design of control law to compensate uncertain dynamics and unmeasurable external disturbances, and the adaptive technique is employed to compensate for the estimation error of the minimum learning parameter method of the neural network to improve the stability of the trajectory tracking system.

Sliding surface $s_u$ can be expressed as

$$s_u = u_e + \lambda_1 \int_0^t u_e(\mu)d\mu \tag{14}$$

where $\lambda_1$ is a positive parameter to be designed. Taking the time derivative of (14) along (10) produces

$$\dot{s}_u = \lambda_1 u_e + \frac{m_{22}}{m_{11}}vr - \frac{d_{11}}{m_{11}}u - \frac{1}{m_{11}}\Delta_u + \frac{1}{m_{11}}\tau_u + \frac{1}{m_{11}}b_u - \dot{\beta}_d \tag{15}$$

Without considering input saturation, the corresponding surge control law can be selected as

$$\tau_{0u} = m_{11}(-\frac{1}{2}s_u\hat{\phi}_u h^T h - \lambda_1 u_e - \frac{m_{22}}{m_{11}}vr + \frac{d_{11}}{m_{11}}u + \dot{\beta}_d + \Phi_u - k_{ue}s_u - \hat{\omega}_u sgn(s_u)) \tag{16}$$

where $k_{ue}$ is a positive parameter to be designed. $\Phi_u$ can be described as

$$\dot{\Phi}_u = \begin{cases} -K_{eu}\Phi_u - \dfrac{|s_u \cdot \Delta\tau_u| + 0.5\Delta\tau_u^2}{\Phi_u^2} \cdot \Phi_u + \Delta\tau_u, & |\Phi_u| \geq \xi_u \\ 0, & |\Phi_u| < \xi_u \end{cases} \tag{17}$$

The meaning of each symbols has the same meanings as those defined in (6). The adaptive law of neural network minimum learning parameter method can be described as

$$\dot{\hat{\phi}}_u = \frac{\Gamma_u}{2}s_u^2 h^T h - \kappa_u \Gamma_u \hat{\phi}_u \tag{18}$$

where $\Gamma_u$ and $\kappa_u$ are parameters to be designed. A robust term is employed to enhance the trajectory tracking system, and its adaptive law can be described as

$$\dot{\hat{\omega}}_u = \gamma_u s_u - \gamma_u \iota_u \hat{\omega}_u \tag{19}$$

where $\gamma_u$ and $\iota_u$ are parameters to be designed. Based on the above analysis, taking into account the input saturation problem, the final surge control law can be described as

$$\tau_u = \begin{cases} \tau_{u\max}, & if\ \tau_{0u} > \tau_{u\max} \\ \tau_{0u}, & if\ \tau_{u\min} \leq \tau_{0u} \leq \tau_{u\max} \\ \tau_{u\min}, & if\ \tau_{0u} < \tau_{u\min} \end{cases} \tag{20}$$

The meaning of each symbols has the same meanings as those defined in (5).

### 4.2 Yaw control law

In this subsection, a second-order sliding mode is introduced into the design of yaw control law to converge the sway tracking error. Similar to the surge control law design process, the role of neural network minimum learning parameter method is to compensate uncertain dynamics and unmeasurable external disturbances, and adaptive technology is employed to improve the robustness of the system.

Sliding surface $s_v$ can be expressed as

$$s_v = \dot{v}_e(t) + \lambda_2 v_e(t) + \lambda_3 \int_0^t v_e(\mu)d\mu \tag{21}$$

where $\lambda_2$ and $\lambda_3$ are parameters to be designed. Taking the time derivative of (21) along (10) produces

$$\dot{s}_v = \ddot{v} - \ddot{v}_d + \lambda_2(\dot{v} - \dot{v}_d) + \lambda_3 v_e \tag{22}$$

where $\ddot{v} = \frac{1}{m_{22}m_{33}}$ $(-m_{11}m_{33}\dot{u}r - m_{11}(m_{11} - m_{22})u^2v + m_{11}d_{22}ur - m_{11}u\tau_r + m_{11}$ $u(\nabla_r - b_r) - m_{33}d_{22}\dot{v} - m_{33}$ $(\dot{\nabla}_v - \dot{b}_v))$, $\ddot{v}_d = v_m - v_n$,

$$v_m = -r[\cos(\psi)\ddot{x}_d + \sin(\psi)\ddot{y}_d] - \sin(\psi)_d + \cos(\psi)_d - r[\cos(\psi)\ddot{x}_d + \sin(\psi)\ddot{y}_d + v_d r - k(\cos(\psi)\dot{x}_e + \sin(\psi)\dot{y}_e)] + k[r\cos(\psi)\dot{x}_e + \sin(\psi)\ddot{x}_e + r\sin(\psi)\dot{y}_e - \cos(\psi)\ddot{y}_e]$$

, $v_n = u_d\frac{\tau_r - d_{33}r + (m_{11} - m_{22})uv}{m_{33}}$. Then, $\dot{s}_v$ can be rewritten as

$$\dot{s}_v = v_b\tau_r + v_v - v_m + \lambda_2(\dot{v} - \dot{v}_d) + \lambda_3 v_e + v_f \tag{23}$$

where $v_b = \frac{(m_{22}u_d - m_{11}u)}{m_{22}m_{33}}$,

$v_v = \frac{-m_{11}m_{33}\dot{u}r - m_{11}(m_{11} - m_{22})u^2v + m_{11}d_{22}ur - m_{33}d_{22}\dot{v} - m_{22}d_{33}ru_d + m_{22}(m_{11} - m_{22})u_d uv}{m_{22}m_{33}}$,

$v_f = \frac{m_{11}u(\nabla_r - b_r) - m_{33}(\dot{\nabla}_v - \dot{b}_v)}{m_{22}m_{33}}$.

***Remark 3*** In the process of yaw control law design, neural shunting model will not be introduced into the design of control strategy to reduce the computational burden of the controller. The reason why neural shunting model is not used to handle $v_d$ is that $\ddot{v}_d$ contains $\tau_r$.

Without considering input saturation, the corresponding yaw control law can be selected as

$$\tau_{0r} = v_b^{-1}(-\frac{1}{2}s_v\hat{\phi}_v h^T h - v_v + v_m - \lambda_2(f_v - \dot{v}_d) - \lambda_3 v_e + \Phi_v - k_{ve}s_v - \hat{\omega}_v sgn(s_v)) \tag{24}$$

where $k_{ve}$ is a positive parameter to be designed. $\Phi_v$ can be described as

$$\dot{\Phi}_v = \begin{cases} -K_{ev}\Phi_v - \dfrac{|s_v \cdot \Delta\tau_r| + 0.5\Delta\tau_v^2}{\Phi_v^2} \cdot \Phi_v + \Delta\tau_r, & |\Phi_v| \geq \xi_v \\ 0, & |\Phi_v| < \xi_v \end{cases} \tag{25}$$

The meaning of each symbols has the same meanings as those defined in (6). The adaptive laws of neural network minimum learning parameter method and robust term are described in (26) and (27), respectively.

$$\dot{\hat{\phi}}_v = \frac{\Gamma_v}{2}s_v^2 h^T h - \kappa_v \Gamma_v \hat{\phi}_v \tag{26}$$

$$\dot{\hat{\omega}}_v = \gamma_v s_v - \gamma_v \iota_v \hat{\omega}_v \tag{27}$$

where $\Gamma_v$, $\kappa_v$, $\gamma_v$ and $\iota_v$ are positive parameters to be designed.

Based on the above analysis, taking into account the input saturation problem, the final yaw control law can be described as

$$\tau_r = \begin{cases} \tau_{r\max}, & if\ \tau_{0r} > \tau_{r\max} \\ \tau_{0r}, & if\ \tau_{r\min} \leq \tau_{0r} \leq \tau_{r\max} \\ \tau_{r\min}, & if\ \tau_{0r} < \tau_{r\min} \end{cases} \tag{28}$$

***Remark 4*** Sign function can undoubtedly add the robustness of the controlled system. However, if $\omega_u$ and $\omega_v$ are selected as constant, this will undoubtedly increase the chattering phenomenon of the control law. So in this paper, an adaptive method is used to estimate the $\omega_u$ and $\omega_v$ values online and in real time to reduce the chattering phenomenon of the control law.

## 5 Stability analysis

The following theorem presents the stability result of the presented trajectory tracking strategy.

Define the following error variable.

$$y_u = \beta_d - u_d \tag{29}$$

whose time derivative along (13) can be expressed by

$$\dot{y}_u = -([A + f(u_d) + g(u_d)]\beta_d - [Bf(u_d) - D(u_d)]) - \mathrm{X}_d \tag{30}$$

where $\mathrm{X}_d = \cos\psi\ddot{x}_d + \sin\psi\ddot{y}_d + v_d r - k\cos\psi\dot{x}_e - k\sin\psi\dot{y}_e$. If $B = D$, (30) can be simplified as (31).

$$y_u = -M\beta_d + Bu_d - \mathrm{X}_d \tag{31}$$

where $M = A + f(u_d) + g(u_d)$.

**Theorem 1** *Consider the trajectory tracking system consisting of the underactuated USV (1) and (2), the control laws (20) and (28), the neural network minimum learning parameter method adaptive laws (18) and (26), the robust term adaptive laws (19) and (27) and the neural shunting model (13). On the premise of optimizing and adjusting parameters* $k$, $\lambda_1$, $\lambda_2$, $\lambda_3$, $\Gamma_u$, $\kappa_u$, $\gamma_u$, $\iota_u$, $\Gamma_v$, $\kappa_v$, $\gamma_v$, $\iota_v$, $k_{ue}$, $k_{ve}$, $K_{eu}$, $K_{ev}$, $\xi_u$, $\xi_v$, *A, B and D, the error signals in the closed-loop system are uniformly ultimately bounded.*

***Proof*** Consider the following Lyapunov function candidate:

$$V = \frac{1}{2}(s_u^2 + s_v^2 + \Gamma_u^{-1}\tilde{\phi}_u^2 + \Gamma_v^{-1}\tilde{\phi}_v^2 + \gamma_u^{-1}\tilde{\omega}_u^2 + \gamma_v^{-1}\tilde{\omega}_v^2 + y_u^2 + \Phi_u^2 + \Phi_v^2) \tag{32}$$

Take the time derivative (31) along (15) and (23), one can get

$$\begin{aligned}\dot{V} &= s_u(\lambda_1 u_e + \frac{m_{22}}{m_{11}}vr - \frac{d_{11}}{m_{11}}u + W_u^T h + \varepsilon_u + \frac{1}{m_{11}}\tau_u - \dot{\beta}_u) \\ &+ s_v(v_b\tau_r + v_v - v_m + \lambda_2 f_v + \lambda_2\frac{1}{m_{22}}(b_v - \nabla_v) - \lambda_2\dot{v}_d + \lambda_3 v_e + v_f) \\ &+ \Gamma_u^{-1}\tilde{\phi}_u\dot{\hat{\phi}}_u + \Gamma_v^{-1}\tilde{\phi}_v\dot{\hat{\phi}}_v + \gamma_u^{-1}\tilde{\omega}_u\dot{\hat{\omega}}_u + \gamma_v^{-1}\tilde{\omega}_v\dot{\hat{\omega}}_v + y_u\dot{y}_u + \Phi_u\dot{\Phi}_u + \Phi_v\dot{\Phi}_v\end{aligned} \tag{33}$$

Submitting the control laws (20), (28) and adaptive laws (18), (19), (26), (27) yields

$$\begin{aligned}\dot{V} \le &- k_{ue}s_u^2 - k_{ve}s_v^2 - \kappa_u\tilde{\phi}_u\hat{\phi}_u - \kappa_v\tilde{\phi}_v\hat{\phi}_v - \iota_u\tilde{\omega}_u\hat{\omega}_u - \iota_v\tilde{\omega}_v\hat{\omega}_v \\ &+ s_u\Phi_u + s_v\Phi_v + s_u\Delta\tau_u + s_v\Delta\tau_v + \Phi_u\dot{\Phi}_u + \Phi_v\dot{\Phi}_v + y_u\dot{y}_u + 1\end{aligned} \tag{34}$$

According to young's inequality analysis (34), one has

$$\begin{aligned}\dot{V} \le &- k_{ue}s_u^2 - k_{ve}s_v^2 - \frac{\kappa_u}{2}\tilde{\phi}_u^2 - \frac{\kappa_v}{2}\tilde{\phi}_v^2 - \frac{\iota_u}{2}\tilde{\omega}_u^2 - \frac{\iota_v}{2}\tilde{\omega}_v^2 \\ &+ s_u\Phi_u + s_v\Phi_v + s_u\Delta\tau_u + s_v\Delta\tau_v + \Phi_u\dot{\Phi}_u + \Phi_v\dot{\Phi}_v + y_u\dot{y}_u \\ &+ \frac{\kappa_u}{2}\phi_u^2 + \frac{\kappa_v}{2}\phi_v^2 + \frac{\iota_u}{2}\omega_u^2 + \frac{\iota_v}{2}\omega_v^2 + 1\end{aligned} \tag{35}$$

If $B = M$, we have $M\beta_d - Mu_d = My_u$. According to Young's inequality, one can get that $-y_u X_d \le \frac{\sigma_u y_u^2}{2} + \frac{X_d^2}{2\sigma_u}$, where $\sigma_u$ is a normal number. Based on the above analysis, (35) can be redefined as

$$\begin{aligned}\dot{V} \le &- k_{ue}s_u^2 - k_{ve}s_v^2 - \frac{\kappa_u}{2}\tilde{\phi}_u^2 - \frac{\kappa_v}{2}\tilde{\phi}_v^2 \\ &- \frac{\iota_u}{2}\tilde{\omega}_u^2 - \frac{\iota_v}{2}\tilde{\omega}_v^2 - (M - \frac{\sigma_u}{2})y_u^2 \\ &+ s_u\Phi_u + s_v\Phi_v + s_u\Delta\tau_u + s_v\Delta\tau_v + \Phi_u\dot{\Phi}_u + \Phi_v\dot{\Phi}_v \\ &+ \frac{\kappa_u}{2}\phi_u^2 + \frac{\kappa_v}{2}\phi_v^2 + \frac{\iota_u}{2}\omega_u^2 + \frac{\iota_v}{2}\omega_v^2 + 1\end{aligned} \tag{36}$$

Besides, noting that $\dot{\Phi}_u\Phi_u = -K_{eu}\Phi_u^2 - \frac{|s_u\Delta\tau_u| + 0.5\Delta\tau_u^2}{\Phi_u^2}\Phi_u^2 + \Delta\tau_u\Phi_u$, $\Delta\tau_u\Phi_u \le \frac{1}{2}(\Delta\tau_u^2 + \Phi_u^2)$, $\dot{\Phi}_v\Phi_v = -K_{ev}\Phi_v^2 - \frac{|s_v\Delta\tau_r| + 0.5\Delta\tau_r^2}{\Phi_v^2}\Phi_v^2 + \Delta\tau_r\Phi_v$, $\Delta\tau_r\Phi_v \le \frac{1}{2}(\Delta\tau_r^2 + \Phi_v^2)$, it follows that

$$\begin{aligned}\dot{V} \le &- k_{ue}s_u^2 - k_{ve}s_v^2 - \frac{\kappa_u}{2}\tilde{\phi}_u^2 - \frac{\kappa_v}{2}\tilde{\phi}_v^2 - \frac{\iota_u}{2}\tilde{\omega}_u^2 - \frac{\iota_v}{2}\tilde{\omega}_v^2 \\ &- (M - \frac{\sigma_u}{2})y_u^2 - (K_{eu} - \frac{1}{2})\Phi_u^2 - (K_{ev} - \frac{1}{2})\Phi_v^2 \\ &+ \frac{\kappa_u}{2}\phi_u^2 + \frac{\kappa_v}{2}\phi_v^2 + \frac{\iota_u}{2}\omega_u^2 + \frac{\iota_v}{2}\omega_v^2 + 1\end{aligned} \tag{37}$$

Define $p_1 = k_{ue}$, $p_2 = k_{ve}$, $p_3 = \frac{\kappa_u}{2}$, $p_4 = \frac{\kappa_v}{2}$, $p_5 = \frac{\iota_u}{2}$, $p_6 = \frac{\iota_v}{2}$, $p_7 = (M - \frac{\sigma_u}{2}) > 0$, $p_8 = (K_{eu} - \frac{1}{2}) > 0$, $p_9 = (K_{ev} - \frac{1}{2}) > 0$, $\Pi = \frac{\kappa_u}{2}\phi_u^2 + \frac{\kappa_v}{2}\phi_v^2 + \frac{\iota_u}{2}\omega_u^2 + \frac{\iota_v}{2}\omega_v^2 + 1$, then (37) becomes

$$\dot{V} \le -p_1 s_u^2 - p_2 s_v^2 - p_3 \tilde{\phi}_u^2 - p_4 \tilde{\phi}_v^2 - p_5 \tilde{\omega}_u^2 - p_6 \tilde{\omega}_v^2 - p_7 y_u^2 - p_8 \Phi_u^2 - p_9 \Phi_v^2 + \Pi \tag{38}$$

Define

$$P = \min\{p_1, p_2, p_3, p_4, p_5, p_6, p_7, p_8, p_9\},$$

then it follows from (38) that

$$\dot{V} \le -2PV + \Pi \tag{39}$$

Solving inequality (39) gives

$$V \le \left(V(0) - \frac{\Pi}{2P}\right)e^{-2lt} + \frac{\Pi}{2P} \le V(0)e^{-2lt} + \frac{\Pi}{2P}, \quad \forall t > 0 \tag{40}$$

Through the above analysis what conclusions can be drawn: $V$ is eventually bounded by $\frac{\Pi}{2P}$, and all error variables in the controlled system are uniformly ultimately bounded. □

## 6 Numerical simulation

In this Section, the simulations of straight-line trajectory tracking and curve trajectory tracking are carried out in the case of disturbance and non-disturbance to verify the correctness and feasibility of the trajectory tracking strategy proposed in this paper. Furthermore, the proposed scheme is compared with [32] and classical PID control strategy to further verify its superiority. CyberShip II USV is selected as the research object, which is developed by the Marine Cybernetics Laboratory in Norwegian University of Science and Technology [33, 34].

### 6.1 Trajectory tracking without disturbance

#### 6.1.1 Straight-line trajectory tracking

The straight-line trajectory tracking task is relatively simple, so the numerical simulation of straight-line trajectory tracking is first performed in this Section. The straight-line trajectory reference can be described as $[x_d = t, y_d = t]$. The initial state of CyberShip II is $[x(0), y(0), \psi(0), u(0), v(0), r(0)] = [15\text{m}, 0\text{m}, 0\text{rad}, 0\text{m/s}, 0\text{m/s}, 0\text{rad/s}]$. The corresponding control parameters are selected as $k = 0.09$, $\lambda_1 = 0.95$, $\lambda_2 = 5$, $\lambda_3 = 0.95$, $\Gamma_u = 0.11$, $\kappa_u = 0.01$, $\gamma_u = 0.12$, $\iota_u = 0.2$, $\Gamma_v = 0.1$, $\kappa_v = 0.011$, $\gamma_v = 0.12$, $\iota_v = 0.03$, $k_{ue} = 0.01$, $k_{ve} = 0.0152$, $K_{eu} = 0.21$, $K_{ev} = 0.12$, $\xi_u = 0.01$, $\xi_v = 0.01$, $A = 2$, $B = 2 + f(u_d) + g(u_d)$ and $D = 2 + f(u_d) + g(u_d)$. The control inputs range of the CyberShip II USV are assumed to be $\tau_{u\max} = 35N$, $\tau_{u\min} = -35N$, $\tau_{r\max} = 35Nm$ and $\tau_{r\min} = -35Nm$. The straight-line trajectory tracking performance without disturbance of the underactuated USV is shown in Figs. 3, 4, 5, 6 and ITAE index (ITAE index refers to the integral of the product of the absolute value of the variable and time) is hired to analyze $x_e$ and $y_e$.

The simulation results of straight-line trajectory tracking without disturbance of the underactuated USV are plotted in Fig. 3, while the tracking errors in X and Y directions are shown in Fig. 4. It can be seen that these three control strategies have good control performance. In addition, since there is no interference, it can be seen from Fig. 4 that the final values of $x_e$ and $y_e$ under the three control strategies are almost zero. Furthermore, it can be seen from Table 1 that the ITAE values of the three control strategies are in the same order of magnitude for both error $x_e$ and $y_e$, and there is a little difference. This is because there is no disturbance in the system, so the control effect is similar. Figs. 5 and 6 depict the comparison curves for control inputs. It can be observed from Fig. 5 that the minimum value of Yu et al. (2012)'s $\tau_u$ is about $-60N$, which has exceeded the range available by the actuator. In addition, it can be seen from Fig. 6 that the extreme value of Yu et al. (2012)'s $\tau_r$ exceeds the maximum value that the actuator can provide. Correspondingly, the $\tau_u$ and $\tau_r$ under the proposed strategy and PID are within the scope of the input that the actuator can provide. In addition, it can be seen that the control input of sliding mode control strategy has a certain chattering phenomenon, which is caused by the principle of sliding mode algorithm.

#### 6.1.2 Curve trajectory tracking

Without changing any control parameters and the initial value of the USV, the curve trajectory tracking is simulated to verify the versatility of the proposed scheme. The reference curve trajectory is a circle with a radius of 20 m, which can be described as

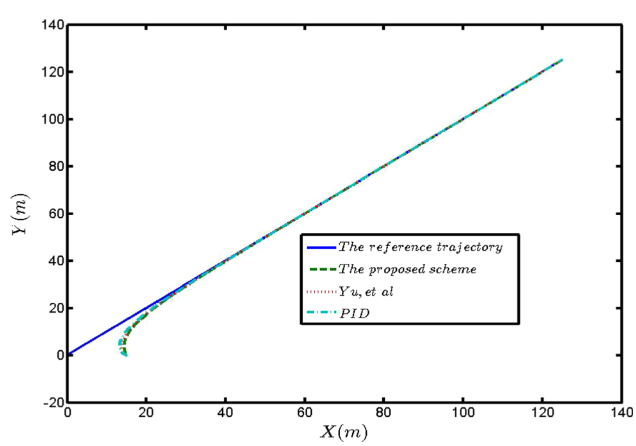


**Fig. 3** The performance of straight-line trajectory tracking without disturbance

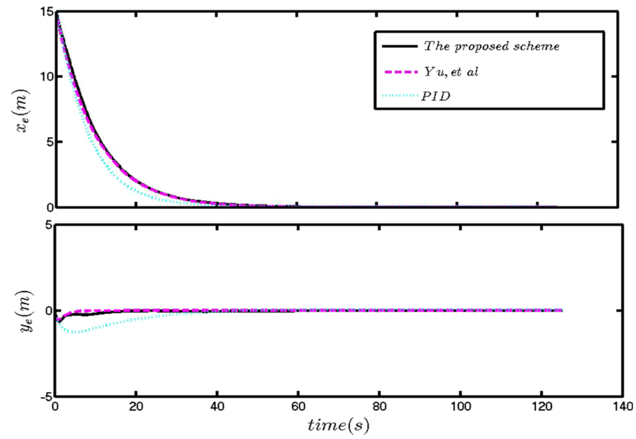


**Fig. 4** The curves of $x_e$ and $y_e$

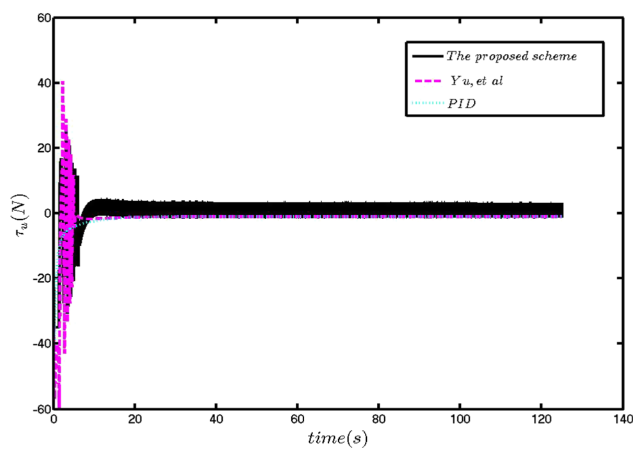


**Fig. 5** The curves of $\tau_u$

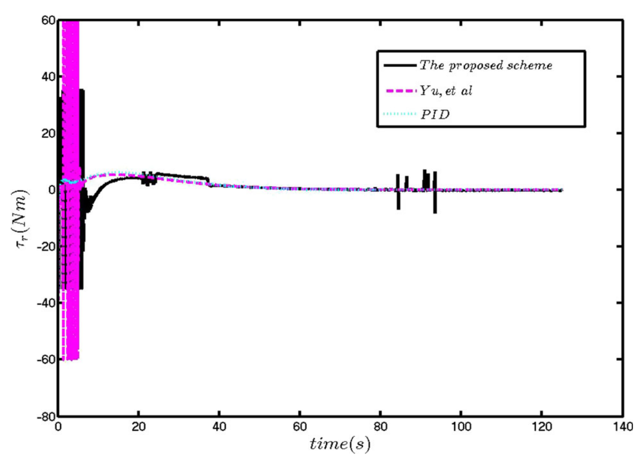


**Fig. 6** The curves of $\tau_r$

$[x_d = 20\cos(0,05t), y_d = 20\sin(0,05t)]$. The curve trajectory tracking performance without disturbance of the underactuated USV is shown in Figs. 7, 8, 9, 10.

**Table 1** ITAE coefficients of $x_e$ and $y_e$

| ITAE | Value | Value | Value |
|---|---|---|---|
| $x_e$ | 1433.1 | 1421.5 | 1399.5 |
| $y_e$ | 54.7 | 84.58 | 99.4 |

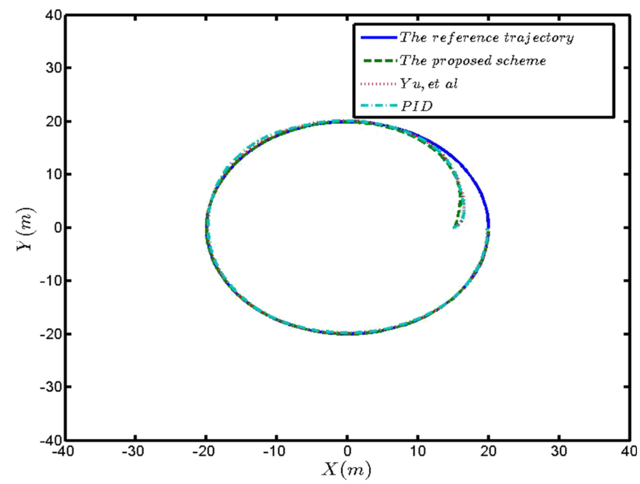


**Fig. 7** The performance of curve trajectory tracking without disturbance

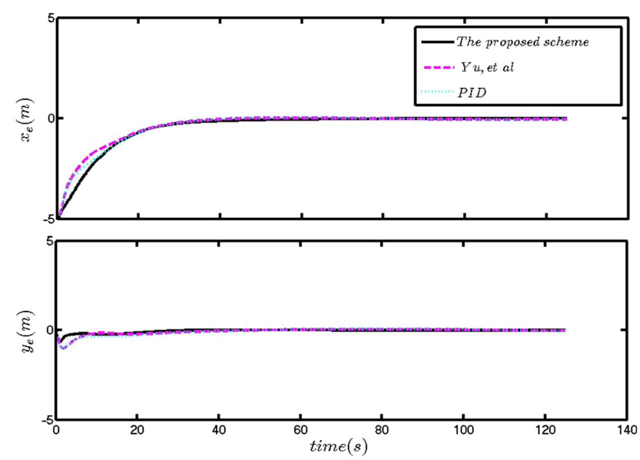


**Fig. 8** The curves of $x_e$ and $y_e$

Fig. 7 depicts the trajectory tracking in a two-dimensional plane, where the reference trajectory is a circle. It can be observed that although any conditions (control parameters and the initial state of USV) have not changed, the curve trajectory tracking still achieves excellent performance. Fig. 8 plots the comparison curves of $x_e$ and $y_e$ in the case of curve trajectory tracking. Because there is no interference, the convergence results of $x_e$ and $y_e$ under the three control strategies are still zero. It can be seen from

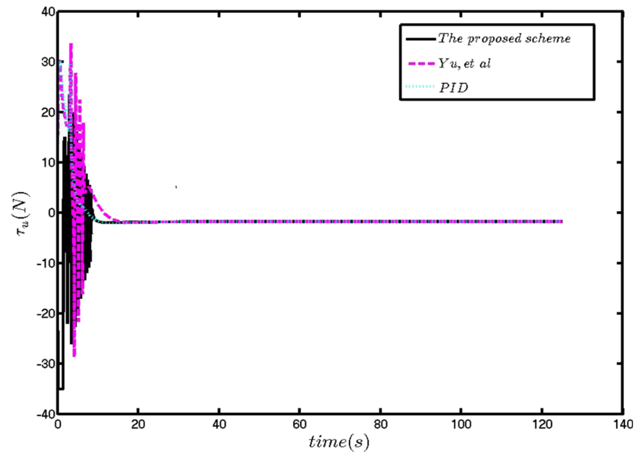


Fig. 9 The curves of $\tau_u$

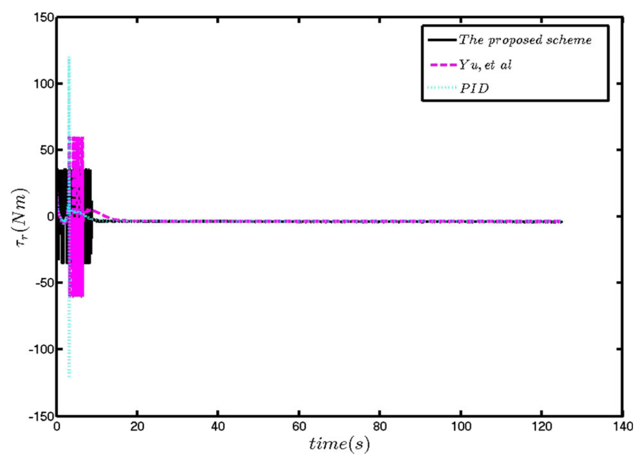


Fig. 10 The curves of $\tau_r$

Table 2 ITAE coefficients of $x_e$ and $y_e$

| ITAE | Value | Value | Value |
|---|---|---|---|
| $x_e$ | 626.1 | 632.5 | 624.8 |
| $y_e$ | 333.7 | 326.2 | 316.9 |

Table 2 that the ITAE values of $x_e$ and $y_e$ under the three control strategies still conform to the law of straight-line trajectory tracking. The comparison curves of $\tau_u$ and $\tau_r$ are shown in Figs. 9 and 10. It reveals that the $\tau_u$ and $\tau_r$ under Yu et al. (2012) and PID control strategies are beyond the maximum range that the actuator can provide at a certain transient. According to the above simulation results, it can be seen that the trajectory tracking performance under the three control strategies is similar, because the cause of interference is not considered.

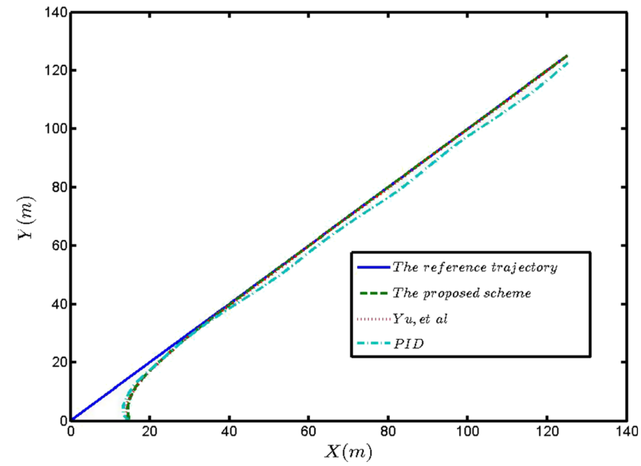


Fig. 11 The performance of straight-line trajectory tracking under disturbance

## 6.2 Trajectory tracking under disturbance

### 6.2.1 Straight-line trajectory tracking

In the actual operating environment of USV, interference is inevitable, so the influence of various interference must be considered in the simulation. Under the same control parameters and USV initial conditions, the straight-line trajectory tracking and curve trajectory tracking are carried out, respectively, and the ITAE index is used to further describe $x_e$ and $y_e$ to reflect the robustness of the proposed control strategy. At the same time, uncertain dynamics and time-varying external disturbances caused by wind, waves and currents are taken as $\Delta_u$=0.2, $\Delta_v$=0.2, $\Delta_r$=0.2, $b_u = 1 + 0.5\sin(0.2t) + 0.3\cos(0.5t)$, $b_v = 1 + 0.5\sin(0.2t) + 0.3\cos(0.4t)$ and $b_r = 1 + 0.2\sin(0.1t) + 0.2\cos(0.2t)$. The straight-line trajectory tracking performance under disturbance of the underactuated USV is shown in Figs. 11, 12, 13, 14.

The straight-line trajectory tracking results under disturbance are plotted in Fig. 11. It is obvious from Fig. 11 that both the proposed scheme and Yu et al. (2012) have good control performance, but PID control effect is not ideal, with obvious error. This is because the proposed scheme and Yu et al. (2012) can compensate for the interference, while PID only relies on its own robustness to suppress the impact of interference. $x_e$ and $y_e$ under the three control strategies are described, and the simulation results are further proved in Fig. 12. It can be seen from Table 3 that the accuracy of the proposed control strategy is the highest, while the trajectory tracking accuracy of PID control is the lowest. Figs. 13 and 14 depict the comparison curves for control inputs. The $\tau_u$ and $\tau_R$ of Yu et al. (2012) exceed the maximum range that the actuator can provide. Although the $\tau_u$ and $\tau_R$ of PID control strategy do

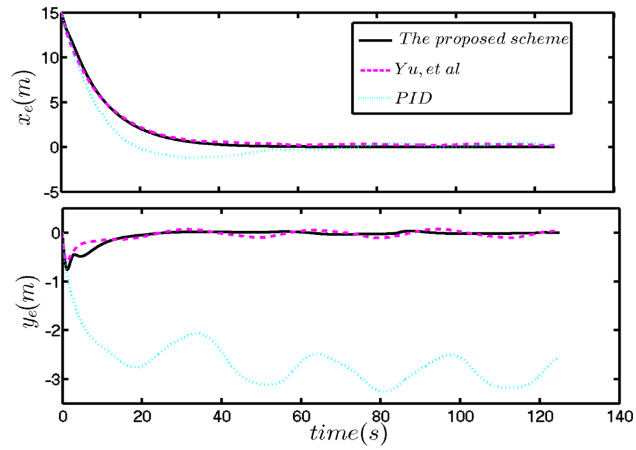


**Fig. 12** The curves of $x_e$ and $y_e$

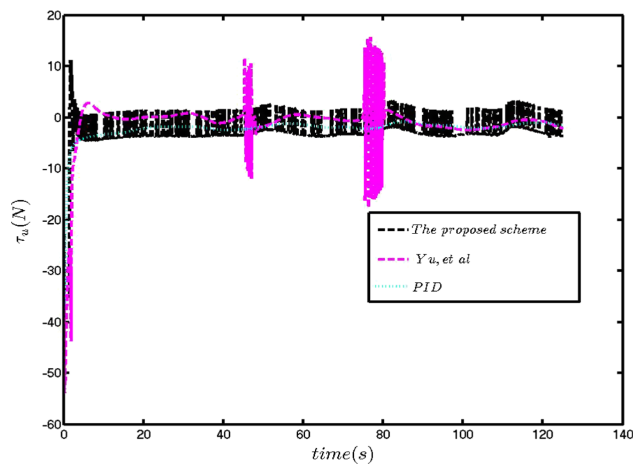


**Fig. 13** The curves of $\tau_u$

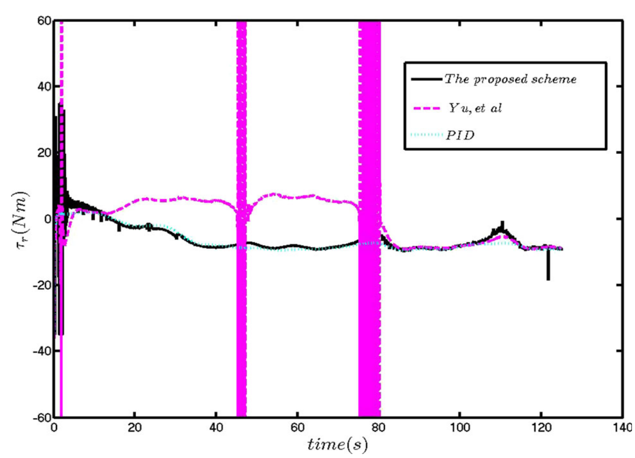


**Fig. 14** The curves of $\tau_r$

not exceed the maximum range that the actuator can provide, the control effect is not ideal.

**Table 3** ITAE coefficients of $x_e$ and $y_e$

| ITAE | Value | Value | Value |
|---|---|---|---|
| $x_e$ | 1544 | 2055 | 3220.1 |
| $y_e$ | 50.75 | 1226.3 | 2211.2 |

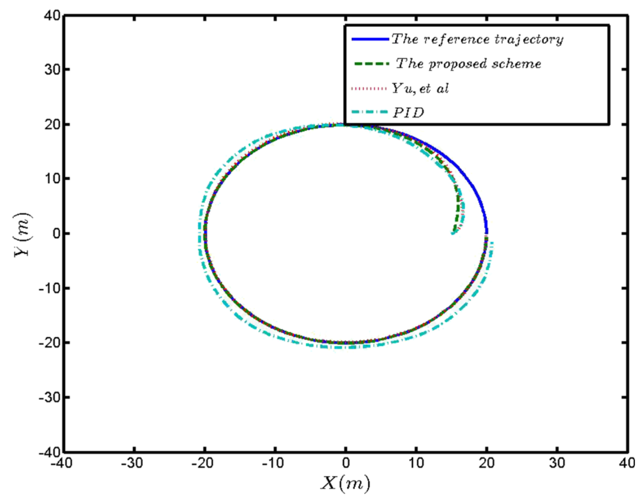


**Fig. 15** The performance of curve trajectory tracking under disturbance

### 6.2.2 Curve trajectory tracking

Similarly, no adjustments are made to any control parameters and other conditions, and the robustness and versatility of the control strategy in this paper are further proved through curve trajectory tracking. The curve trajectory tracking performance under disturbance is shown in Figs. 15, 16, 17, 18.

Figure 15 shows the results of circular trajectory tracking with three control strategies in the presence of interference. It is obvious that the proposed control strategy and Yu et al. (2012) have good control performance, while the simulation under PID strategy has large error. Fig. 16 and Table 4 further verify the simulation results. The comparison curves of $\tau_u$ and $\tau_r$ are shown in Figs. 17 and 18. Both Yu et al. (2012) and PID control strategies have control inputs that exceed the maximum range that the actuator can provide. In summary, the robustness and generality of the proposed trajectory tracking control strategy are proved through the simulation of straight-line trajectory tracking and curve trajectory tracking without disturbance and with disturbance.

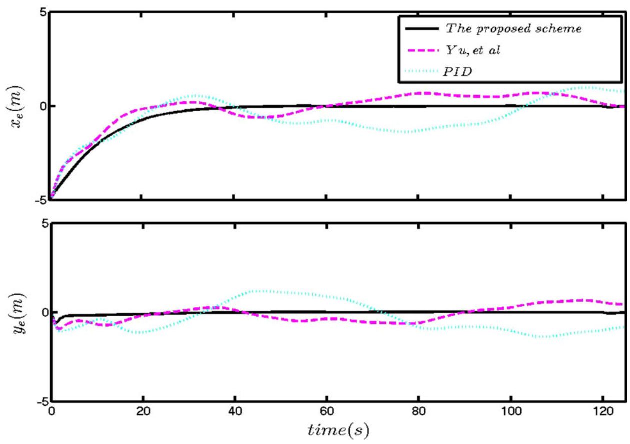


**Fig. 16** The curves of $x_e$ and $y_e$

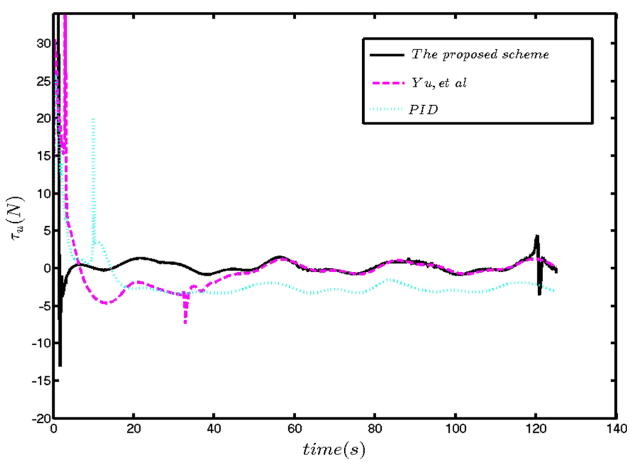


**Fig. 17** The curves of $\tau_u$

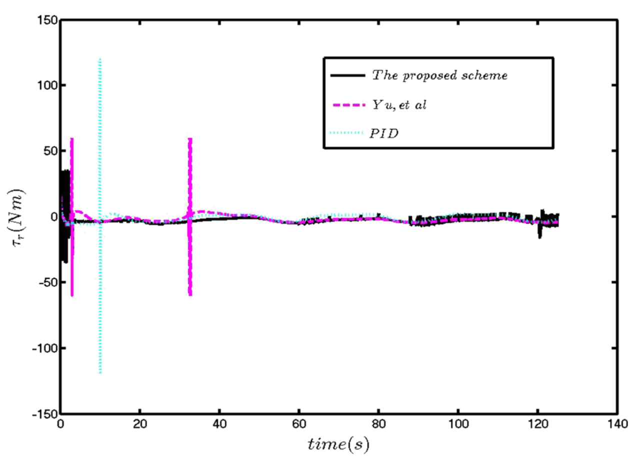


**Fig. 18** The curves of $\tau_r$

**Table 4** ITAE coefficients of $x_e$ and $y_e$

| ITAE | Value | Value | Value |
|---|---|---|---|
| $x_e$ | 586.8 | 3378.1 | 6441.5 |
| $y_e$ | 149.4 | 3201.7 | 7023.4 |

## 7 Conclusion

This paper has proposed a practical adaptive trajectory tracking control strategy for an underactuated USV. The proposed scheme is proposed by combing a first-order sliding mode, a second-order sliding mode, neural shunting model, minimum learning parameter method for neural network and adaptive technology. Neural shunting model and minimum learning parameter method can reduce the computational burden of the controller to some extent. Finally, the feasibility and superiority of the proposed tracking scheme are verified by the simulation experiments of straight-line and curve.

Although this paper takes many practical situations into account, there are still many problems to be solved. For example, the proposed trajectory tracking control strategy does not take the dynamic characteristics of the actuator into account. In other words, the final control output is force $\tau_u$ and torque $\tau_r$, rather than propeller speed and corresponding rudder angle, which is difficult to achieve in engineering. Therefore, in the future research, the author plans to consider the dynamic characteristics of the actuator in the design of the controller and carries out the field experiment if conditions permit.

**Acknowledgements** The authors would like to thank the reviewers for their constructive comments, which have improved the quality of this paper. This work was supported in part by National Natural Science Foundation of China under Grant 51609033, Natural Science Foundation of Liaoning Province under Grant 20180520005, the Key Development Guidance Program of Liaoning Province of China under Grant 2019JH8/10100100, the Soft Science Research Program of Dalian City of China under Grant 2019J11CY014 and Fundamental Research Funds for the Central Universities under Grant 3132021106, 3132019005, 3132019311.

## Declarations

**Conflicts of interest** The authors declare there is no conflicts of interest regarding the publication of this paper.

## References

1. Mousazadeh H, Jafarbiglu H, Abdolmaleki H, Omrani E, Monhaseri F, Abdollahazdeh M, Mohammadi-Aghdam A, Kiapei A, Salmani-Zakaria Y, Makhsoos A (2018) Developing a navigation, guidance and obstacle avoidance algorithm for an unmanned surface vehicle (USV) by algorithms fusion. Ocean Eng 159:56–65

2. Chen X, Liu Z, Zhang J, Zhou D, Dong J (2019) Adaptive sliding-mode path following control system of the underactuated USV under the influence of ocean currents. J Syst Eng Electron 29(6):1271–1283
3. Kim H, Yun S, Choi Y, Ryu J, Suh J (2020) Improved dynamic window approach with ellipse equations for autonomous navigation of unmanned surface vehicle. J Inst Control 26(8):624–629
4. Asfihani T, Subchan S, Rosyid DM (2019) Dubins path tracking controller of USV using model predictive control in sea field. J Eng Appl Sci 14(20):7778–7787
5. Xia K, Gao H, Ding L, Liu G, Deng Z, Liu Z, Ma C (2018) Trajectory tracking control of wheeled mobile manipulator based on fuzzy neural network and extended Kalman filtering. Neural Comput Appl 30(2):447–462
6. Elmokadem T, Zribi M, Youcef K (2016) Trajectory tracking sliding mode control of underactuated AUVs. Nonlinear Dyn 84(2):1079–1091
7. Liu C, Zou Z, Li T (2015) Path following of underactuated surface vessels with fin roll reduction based on neural network and hierarchical sliding mode technique. Neural Comput Appl 26(7):1525–1535
8. Stateczny A, Burdziakowski P, Najdecka K, Stateczna BD (2020) Accuracy of trajectory tracking based on nonlinear guidance logic for hydrographic unmanned surface vessels. Sensors 20(3):1–16
9. Ghommam J, Iftekhar L, Saad M (2019) Adaptive finite time path-following control of underactuated surface vehicle with collision avoidance. J Dyn Syst Meas Control 141(12):121008
10. Bibuli M, Bruzzone G, Caccia M, Lapierre L (2009) Path following algorithms and experiments for an unmanned surface vehicle. J Field Robot 26(8):669–688
11. Godhavn J (1996) Nonlinear tracking of underactuated surface vessels. In: Proceeding IEEE Conference on Decision & Control Kobe, 975-980
12. Ghommam J, Mnif F, Derbel N (2010) Global stabilisation and tracking control of underactuated surface vessels. IET Control Theory Appl 4(1):71–88
13. Yang Y, Du J, Liu H, Guo C, Abraham A (2014) A trajectory tracking robust controller of surface vessels With disturbance uncertainties. IEEE Trans Control Syst Technol 22(4):1511–1518
14. Park B, Yoo S (2019) Adaptive-observer-based formation tracking of networked uncertain underactuated surface vessels with connectivity preservation and collision avoidance. J Frankl Inst 356(15):7947–7966
15. Haseltalab A, Negenborn RR (2019) Adaptive control for autonomous ships with uncertain model and unknown propeller dynamics. Control Eng Pract 91(10):104116.1-104116.12
16. Abbasi SMM, Jalali A (2020) Fuzzy tracking control of fuzzy linear dynamical systems. ISA Trans 97:102–115
17. Yen VT, Nan WY, Cuong PV (2019) Recurrent fuzzy wavelet neural networks based on robust adaptive sliding mode control for industrial robot manipulators. Neural Comput Appl 31(11):6945–6958
18. Li JH, Lee PM, Jun BH, Lim YK (2008) Point-to-point navigation of underactuated ships. Automatica 44(12):3201–3205
19. Qin H, Li C, Sun Y (2020) Adaptive neural network-based fault-tolerant trajectory-tracking control of unmanned surface vessels with input saturation and error constraints. IET Intell Transp Syst 14(5):356–363
20. Zhang G, Zhang X, Zheng Y (2015) Adaptive neural path-following control for underactuated ships in fields of marine practice. Ocean Eng 104:558–567
21. Yang Y, Li T, Wang X (2006) Robust adaptive neural network control for strict-feedback nonlinear systems via small-gain approaches, International Symposium on Neural Networks. Springer, Berlin, Heidelberg, pp 888–897
22. Mu D, Wang G, Fan Y (2017) Design of adaptive neural tracking controller for Pod propulsion unmanned vessel subject to unknown dynamics. J Electr Eng Technol 12(6):2365–2377
23. Li Y, Tong S, Li T (2016) Hybrid fuzzy adaptive output feedback control design for uncertain MIMO nonlinear systems with time-varying delays and input saturation. IEEE Trans Fuzzy Syst 24(4):841–853
24. Zhou Q, Wang L, Wu C, Li H, Du H (2017) Adaptive fuzzy control for nonstrict-feedback systems with input saturation and output constraint. IEEE Trans Syst Man Cybern Syst 47(1):1–12
25. Chwa D (2011) Global tracking control of underactuated ships with input and velocity constraints using dynamic surface control method. IEEE Trans Control Syst Technol 19(6):1357–1370
26. Lekkas AM, Fossen TI (2014) Integral LOS path following for curved paths based on a monotone cubic hermite spline parametrization. IEEE Trans Control Syst Technol 22(6):2287–2301
27. Pan CZ, Lai XZ, Yang SX, Wu M (2015) A biologically inspired approach to tracking control of underactuated surface vessels subject to unknown dynamics. Expert Syst Appl 42(4):2153–2161
28. Yang Y, Zhou C, Jia X (2002) Robust adaptive fuzzy control and its application to ship roll stabilization. Inf Sci 142(1–4):177–194
29. Chen M, Ge SS, Ren B (2011) Adaptive tracking control of uncertain MIMO nonlinear systems with input constraints. Automatica 47(3):452–465
30. Yen VT, Nan WY, Cuong PVL (2019) Recurrent fuzzy wavelet neural networks based on robust adaptive sliding mode control for industrial robot manipulators. Neural Comput Appl 31(11):6945–6958
31. Van M (2019) An enhanced tracking control of marine surface vessels based on adaptive integral sliding mode control and disturbance observer. ISA Trans 90:30–40
32. Yu R, Zhu Q, Xia G, Liu Z (2012) Sliding mode tracking control of an underactuated surface vessel. IET Control Theor Appl 6(3):461–466
33. Skjetne R, Smogeli, $\phi$, Fossen TI (2004) Modeling, identification, and adaptive maneuvering of Cybership II: a complete design with experiments. In: Proc. IFAC Conf. Control Appl. Marine Syst, 203-208
34. Alfaro CE, Mcgookin EW, Murray SDJ, Fossen TI (2008) Genetic programming for the automatic design of controllers for a surface ship. IEEE Trans Intell Transp Syst 9(2):311–321